Design, Development and Integration of Novel Antennas for Miniaturized UHF RFID Tags

Amin H. Rida, *Student Member, IEEE*, Li Yang, *Student Member, IEEE*, S. Serkan Basat, Antonio Ferrer-Vidal, Symeon (Simos) Nikolaou, and Manos M. Tentzeris, *Senior Member, IEEE*

***Abstract*—An overview of design requirements and novel approaches for improved performance UHF radio frequency identification (RFID) tags is presented. Two matching techniques, an inductively coupled structure and a serial stub structure are discussed. Different miniaturized antenna topologies are proposed, focusing on low-profile, high efficiency and high directivity in very compact (less than 3 in $\times$ 3 in) configurations.**

***Index Terms*—Inductively coupled matching, low-profile antennas, printed-antennas, RFID, serial stub matching, UHF.**

I. Introduction

The demand for flexible RFID tags has recently increased tremendously due to the requirements of automatic identification in various areas, such as item-level tracking, access control, electronic toll collection and vehicle security [1]. Compared with the lower frequency tags (LF and HF bands) already suffering from limited read range (1–2 feet), RFID tags in UHF band see the widest use due to their higher read range (over 10 feet) and higher data transfer rate [2]. Three major challenges exist in today's RFID technologies that could potentially impede their practical implementation. One is the design of small-size tag antennas with very high efficiency and effective impedance matching for IC chips with typically high capacitive reactance [3]. These antenna requirements are essential to optimize the RFID system power-performance, especially for passive or semi-active configurations, where the only energy source is the incoming reader energy. Another major challenge is the realization of ultra-low-cost RFID tags, with a cost requirement for individual tags below one cent [4]. The third obstacle is the existence of various different UHF frequency bands ranging from 860 to 950 MHz for Europe (866 $\rightarrow$ 868 MHz), Asia (864 $\rightarrow$ 964 MHz) and US (902 $\rightarrow$ 928 MHz). The universal operation of the RFID's necessitates the use of wideband antennas covering all three bands.

In this paper, various novel approaches in adaptive impedance matching, radiation efficiency, and miniaturization method are proposed. These approaches are supplemented with modeling, simulation, and measurement results.

Manuscript received September 08, 2008; revised March 31, 2009. First published July 14, 2009; current version published November 04, 2009.

A. H. Rida, L. Yang, and M. M. Tentzeris are with the Department of Electrical and Computer Engineering, Georgia Institute of Technology, Atlanta, GA 30308 USA (e-mail: arida@gatech.edu; liyang@ece.gatech.edu; etentze@ece.gatech.edu).

S. Serkan Basat was with the Department of Electrical and Computer Engineering, Georgia Institute of Technology, Atlanta, GA 30308 USA. He is now with Motorola Inc., Plantation, FL 33322 USA (e-mail: sabri.basat@motorola.com).

A. Ferrer-Vidal was with the Department of Electrical and Computer Engineering, Georgia Institute of Technology, Atlanta, GA 30308 USA. He is now in Barcelona, Spain.

S. Nikolaou was with the Department of Electrical and Computer Engineering, Georgia Institute of Technology, Atlanta, GA 30308 USA. He is now with Frederick University, Nicosia 1036, Cyprus and also with the Frederick Research Center, Nicosia 1036, Cyprus (e-mail: s.nikolaou@frederick.ac.cy).

Color versions of one or more of the figures in this paper are available online at http://ieeexplore.ieee.org.

Digital Object Identifier 10.1109/TAP.2009.2027347

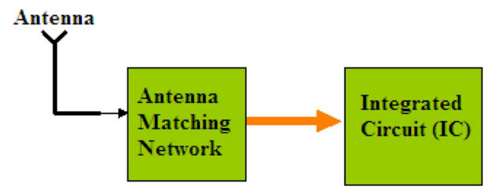

Fig. 1. Block diagram of a passive RFID tag.

II. Serial Stub Feed Structure

A. Design

A major challenge in RFID antenna design is the impedance matching of the antenna (Z_{ANT}) to that of the IC (Z_{IC}). For years, antennas have been designed primarily to match either 50 Ω or 75 Ω loads. However, RFID chips primarily exhibit complex input impedance, making matching extremely challenging. Among other challenges are: compact antenna size, low cost, omni-coverage (omnidirectional antenna pattern), long read range, and wide bandwidth. Most available commercial RFID tags are passive due to cost and fabrication requirements. A block diagram of a passive RFID tag is shown in the Fig. 1 below. The antenna matching network must provide the maximum power delivered to the IC which is used to store the data that is transmitted to/received from the reader.

In this design approach, a very compact configuration (in an area less than 3 in $\times$ 3 in) of a $(\lambda/2)$ dipole antenna was developed, where λ is the free space wavelength. The $(\lambda/2)$ antenna design is favorable for its quasi- omnidirectional radiation pattern; a fundamental requirement for RFID's to allow for the communication between the RFID tags and the RFID reader, independent of the orientation of the tags. The step by step design is illustrated in the figures below. Fig. 2(a) shows the main radiating element which if stretched from one end to the other corresponds to a length of $\sim$16 cm (which is $\lambda/2$ around the center frequency 935 MHz in air). The tapering of the antenna was chosen for maximum current flow (hence optimum efficiency) and to achieve a high bandwidth. The $\lambda/2$ antenna was folded

0018-926X/$26.00 © 2009 IEEE

Authorized licensed use limited to: Georgia Institute of Technology. Downloaded on November 29, 2009 at 22:44 from IEEE Xplore. Restrictions apply.

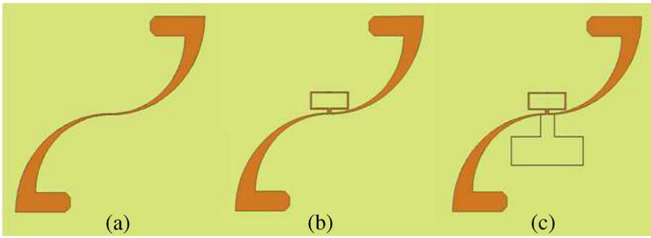

Fig. 2. Step by step antenna design showing: (a) radiating body, (b) radiating body plus double inductive stub , (c) final antenna structure with the resistive stub.

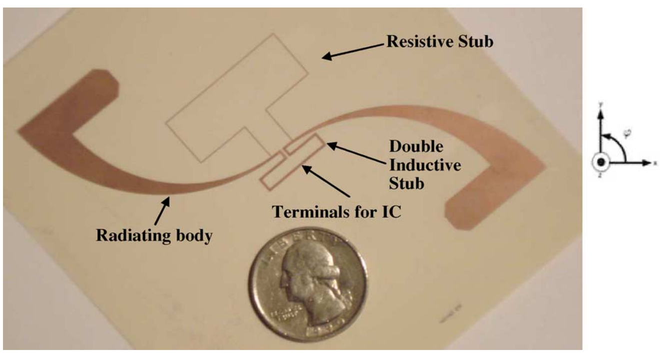

Fig. 3. RFID antenna structure showing stubs.

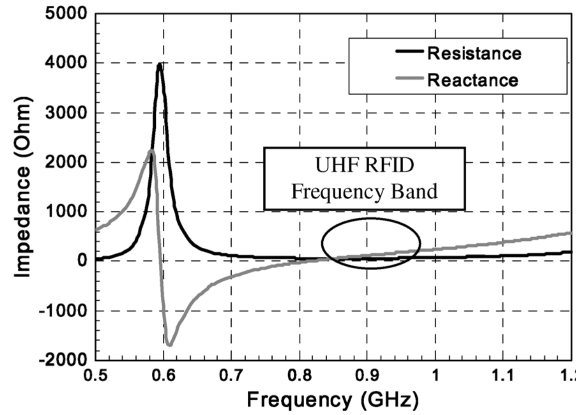

Fig. 4. Simulated input impedance of the S-shaped antenna.

as shown in Fig. 2 at a distance $(\sim 0.16\lambda)$ not to cause any significant current perturbation (keeping maximum radiation efficiency), while making the design more compact. Without loss of generality, in this design the overall matching network is designed to conjugately match an RFID chip with a high capacitive impedance of $\mathrm{Z_{IC}} = 73 - \mathrm{j}113\ \Omega$. Fig. 2 also shows the step by step procedure used in the design. To satisfy the conformality RFID requirements, the proposed antenna was fabricated on flexible 4-mil Liquid Crystal Polymer (LCP) that is an organic material which has a dielectric constant ε_{r} of ∼3.10 and a loss tangent $(\tan\delta)$ of 0.0019 [5].

The IC used for this design has four ports; two input ports namely RF1 and RF2 which may be connected to a single or dual antenna configuration, one ground port $(\mathrm{V_{ss}})$ to connect to the second arm of the antenna (for example in the dipole-based design of this paper) and an open port $(\mathrm{V_{dd}})$ to measure or drive the bias voltage of the IC when conducting measurements. The two input ports are identical and can be used either for single or dual antenna topologies. For single antenna structures RF2 and $\mathrm{V_{ss}}$ ports are shorted. The resistive shorting stub and the double inductive stub as illustrated in Fig. 3 constitute the overall matching network. The resistive stub is used to tune the resistance of the antenna to match that of the IC. In this design the size and shape (thin long loop shaped line) of the resistive stub were designed to have an optimum match to $\mathrm{Z_{IC}} = 73 - \mathrm{j}113\ \Omega$. The double inductive stub is composed of two inductive stubs to provide symmetry on both sides of the antenna. The double inductive stub also serves as the reactive tuning element of the antenna.

The feeding point of the antenna is at the bottom part of the double inductive stub where an IC would be surface mounted. Fig. 3 illustrates the final structure.

The stubs were designed to have a center frequency $\mathrm{f_0}$ at 895 MHz with a bandwidth of 70 MHz operating from 860 → 930 MHz (European and U.S. frequencies). A wide frequency sweep has also been performed up to 5 GHz where no parasitic radiation has been observed for this antenna. Those variables can be fine tuned to optimize the antenna characteristics on the RFID tag at any frequency and matched to any IC impedance.

The structure was simulated and optimized in the system level design tool HFSS. The input impedance of the simulated antenna design is shown in Fig. 4. As it can be observed the RFID UHF band (860 → 930 MHz) is outside the antenna self-resonance peak, resulting in a more flat impedance response against frequency. This yields to a bandwidth of ∼8% which is predominantly realized by the finite slope of the reactance of the antenna in the frequency of interest.

The simulated impedance at the center frequency $\mathrm{f_0} = 895\ \mathrm{MHz}$ is $57.46 + \mathrm{j}112.1$ which results in an $\mathrm{S_{11}} < -18$ dB. This antenna has a bandwidth of ∼8% (70 MHz) where the bandwidth is defined by a voltage standing wave ratio (VSWR) of 2 (alternatively a $\mathrm{S_{11}}$ of -9.6 dB) as shown under the measurement section (Fig. 12). The tapering of this S-shaped antenna along with the matching techniques (resistive and inductive stubs) allow for the first-ever 3 in $\times$ 3 in RFID antenna with such a high bandwidth (∼8%).

The reflection coefficient or $\mathrm{S_{11}}$ of this antenna was calculated based on the power S11 which takes into account the capacitance of the IC [6]

$$|s^2| = \left|\frac{Z_{IC} - Z_{\mathrm{ANT}}^*}{Z_{IC} - Z_{\mathrm{ANT}}}\right|^2.$$

$\mathrm{Z_{IC}}$ represents the impedance of the IC and $\mathrm{Z_{ANT}}$ represents the impedance of the antenna with $\mathrm{Z_{ANT}^*}$ being its conjugate.

The simulated radiation pattern and radiation efficiency were numerically computed in HFSS by introducing an RLC boundary along with the port impedance that simulates the behavior of the IC (with its complex impedance feed). In Fig. 5 the 2-D radiation plot is shown for the $\mathrm{phi} = 0^\circ$ and $\mathrm{phi} = 90^\circ$ (as defined in Fig. 2) where an omnidirectional pattern is realized. The radiation pattern throughout the bandwidth of the antenna has also shown to have an omnidirectional pattern similar to that of a classic $(\lambda/2)$ dipole antenna.

Authorized licensed use limited to: Georgia Institute of Technology. Downloaded on November 29, 2009 at 22:44 from IEEE Xplore. Restrictions apply.

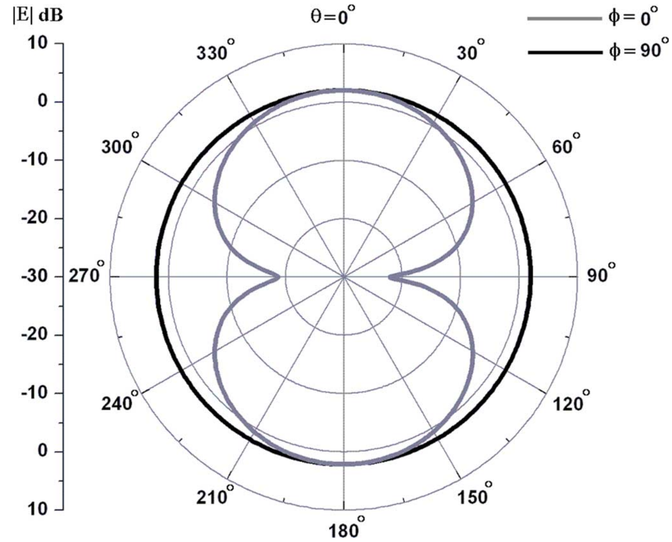

Fig. 5. 2D far-field radiation plot.

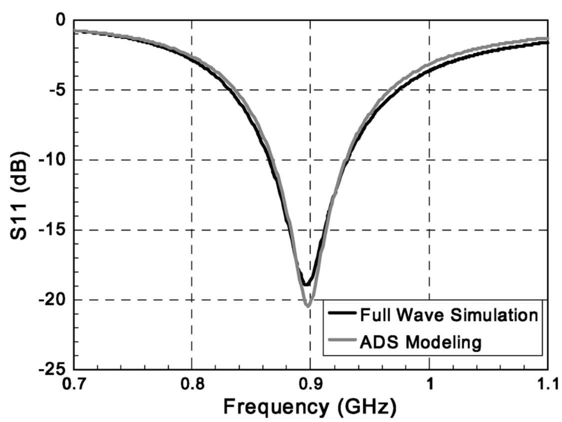

Fig. 6. S_{11} for the exact structure and for the equivalent circuit model.

A directivity of 2.10 dBi is achieved with a radiation efficiency of 97%. The omnidirectional radiation is one of the most fundamental requirements for RFID's to allow for their reading/writing operation independent of the orientation of their antenna with respect to the reader. Preliminary experimental results have verified the shape of Fig. 5 theoretical ones.

B. UHF RFID Antenna Modeling

In order to obtain a thorough understanding of the power reflection caused by any mismatch at the terminals of the feed structure of the antenna, a wideband equivalent circuit model has been developed. This model serves as a benchmark for the design of an RFID antenna to theoretically match any Z_{IC} for maximum power flow resulting in optimum antenna efficiency and an excellent read range.

Based on a physical approach, an equivalent lumped element circuit model was derived. The system level design and simulation tool advanced design system (ADS) was used to simulate the behavior of the circuit model (S_{11} parameter) and resulted in a negligible error function $(< 10^{-5})$. Fig. 6 below shows the agreement between the lumped element circuit S parameters with that of the structure (from the full wave simulator).

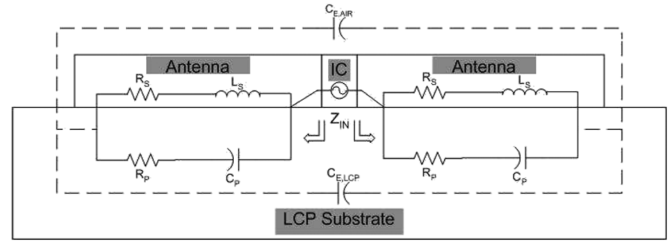

Fig. 7. Cross-sectional detail showing equivalent lumped element model of RFID antenna shown in Fig. 2(a) and (b).

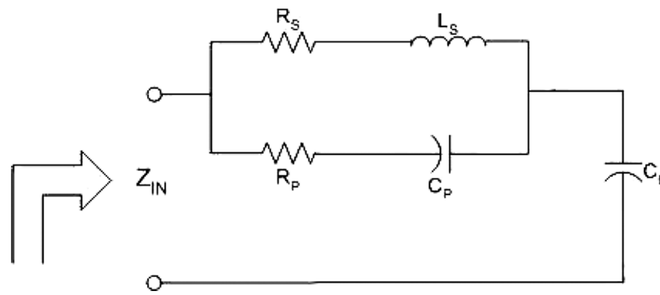

Fig. 8. Equivalent circuit model of RFID antenna shown in Fig. 2(a) and (b).

Fig. 7 shows the detailed equivalent circuit of the radiating body only. Each arm of the radiating body consists of a resistor in series with an inductor, the combination of which models the metal effects. A capacitor in series with a resistor, which are located in parallel with the previous combination of L_s and R_s model the substrate effects. Finally, the capacitive coupling or E-Field coupling between the two arms of the S-shaped antenna is modeled by the top and bottom capacitors (for air and dielectric capacitive coupling respectively). This lumped element model covers a frequency range 700 $\rightarrow$ 1100 MHz as shown in Fig. 6 above.

The circuit configuration in Fig. 7 can be simplified to the one shown in Fig. 8 by using symmetry and direct circuit analysis.

Since the double inductive stub is connected in series with the radiating body (the antenna is now fed in the center of the double inductive stub), the equivalent circuit model of the second stage design (radiating body plus inductive stub) as shown in Fig. 2 has the same circuit elements configuration as the one in Fig. 8, with change in values only. The final stage of the design has the circuit model configuration shown in Fig. 9. Due to the configuration of the resistive shorting stub (connected in parallel with the radiating body plus inductive stub), the components: $R_{s2}, L_{s2}, R_{p2}, C_{p2}$ are introduced as shown in Fig. 8 below and model the same effects as those discussed previously for radiating body circuit model (Fig. 8).

The equivalent circuit shows how stubs can be used to tune the impedance in order to match to any IC. Parametric sweeps can be used along different stubs structures (for example loops structures can be used for adding series inductance or parallel capacitance). The resistance of the antenna is mainly determined by the radiating body and can be tuned by the two stubs as shown above. This model also helps to determine the amount of loss (as parallel resistance and capacitance) due to the substrate loss which helps in understanding radiation efficiency as a function of the substrate.

Authorized licensed use limited to: Georgia Institute of Technology. Downloaded on November 29, 2009 at 22:44 from IEEE Xplore. Restrictions apply.

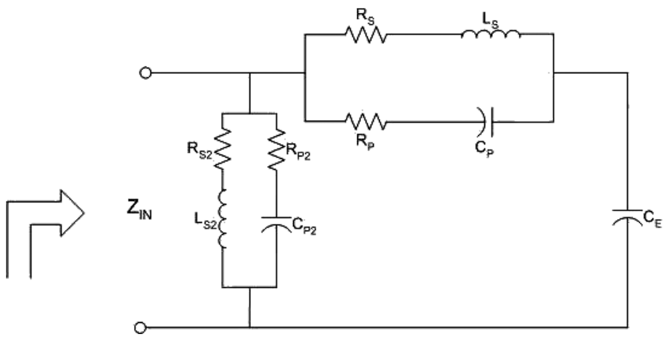

Fig. 9. Equivalent circuit for antenna structure shown in Fig. 2(c).

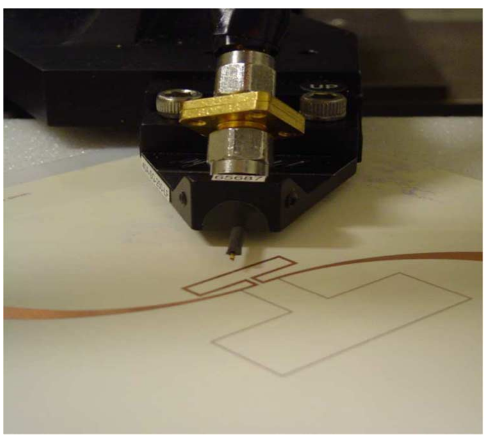

Fig. 10. Photograph of the probe plus S-shaped antenna.

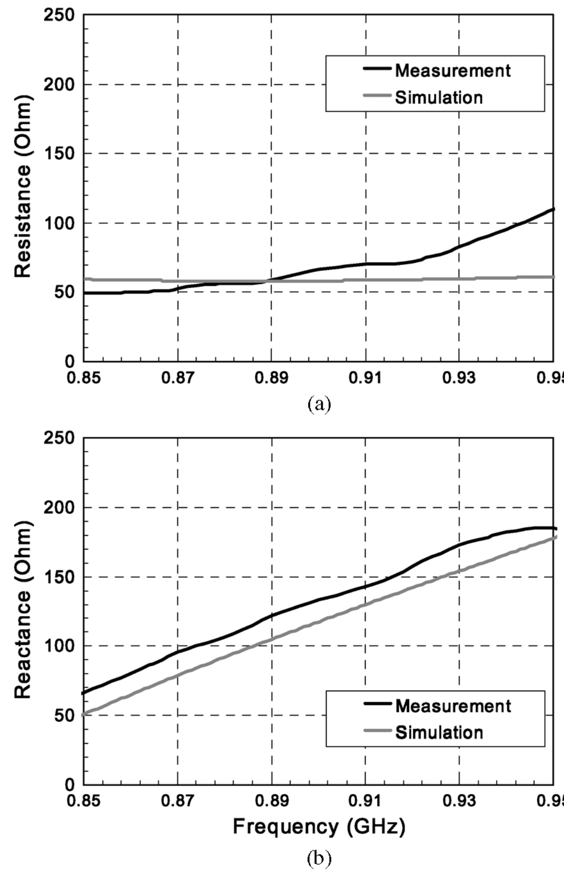

Fig. 11. Measured and simulated data of input impedance: (a) Resistance and (b) reactance.

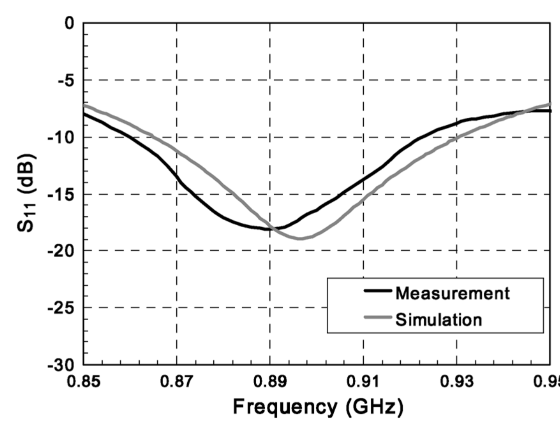

Fig. 12. S_{11} for measured and simulated data.

C. Measurements

In order to accurately measure the input impedance of the RFID antennas, numerous problems should be taken into consideration. First of all, a traditional probe station was not suitable for our tests due to the undesired shorting effect of the metallic chuck, which was behaving as a spurious ground plane for the dipole antennas. To tackle the problem, a custom-made probe station using wood and high density polystyrene foam was built. This type of foam was selected due to its low dielectric constant (1.06) [7] resembling that of the free space. A photograph of the probe measurement setup is shown in Fig. 10. A $5 \cdot \lambda/2$-thick foam station was designed in order to ensure minimum backside reflections of the antenna.

It was also taken into account the fact that the antennas were balanced structures and a typical GS probe connected to a regular coaxial cable would provide an unbalanced signal. To prevent a current difference between the dipole arms, a $\lambda/4$ balun with an operational bandwidth of $840 \rightarrow 930$ MHz (which covers the band of interest for this design) was used. After all the above mentioned precautions were taken and minding about the calibration process, S parameters were measured with an Agilent 8510C S parameter receiver and transformed to Z_{IN} or Z_{ANT}.

Fig. 11 and Fig. 12 show a very good agreement between the simulated results and the measurements for the antenna input impedance and S_{11} parameter respectively. The demonstrated antenna bandwidth allows for a universal operation of the proposed UHF RFIDs (Worldwide frequency coverage except Japan and some Asian countries that operate at a frequency of 950 MHz and higher).

D. Effect on Antenna Parameters When Placed on Common Packaging Materials: Papers and Plastics

In order to fully investigate the effect of the surroundings on the antenna parameters, such as the resonance, bandwidth, and radiation, the s-shaped antenna was simulated for three practical configurations: on a 4 mm thick common plastic material [PET-Polyethylene terephthalate ($\varepsilon_r = 2.25$ and $\tan\delta = 0.001$)], on 4 mm thick paper ($\varepsilon_r = 3.28$ and $\tan\delta = 0.006$

Authorized licensed use limited to: Georgia Institute of Technology. Downloaded on November 29, 2009 at 22:44 from IEEE Xplore. Restrictions apply.

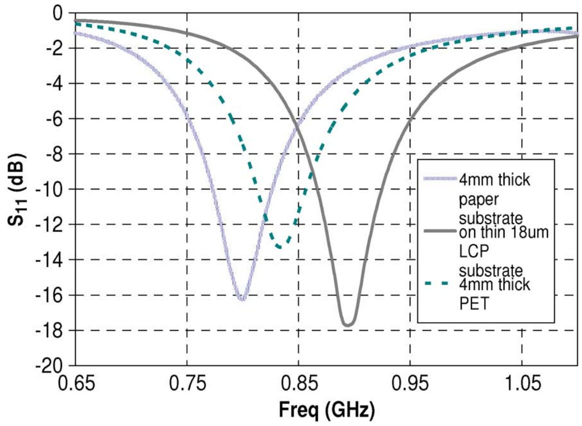

Fig. 13. S_{11} for 4 mm thick paper and PET substrates.

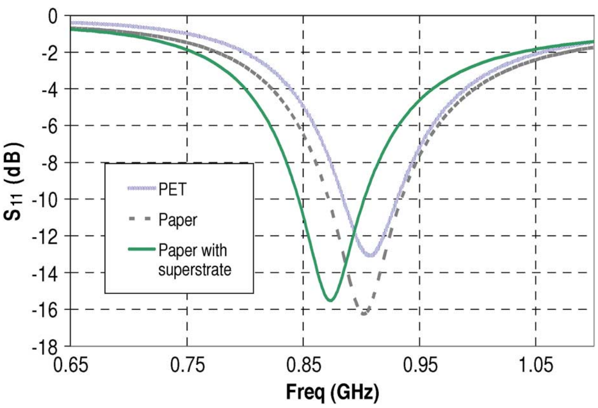

Fig. 14. S_{11} for 4 mm thick paper and PET substrates with modified antenna dimensions.

[8]) substrate as well in an embedded structure with 0.5 mm thick paper superstrate on a 4 mm paper substrate. Fig. 13 shows the Reflection coefficient or S_{11} results for the polyethylene and paper substrates. As seen in the figure, a shift in resonance frequency occurs (95 MHz for paper and 60 MHz for PET from the original antenna with center frequency 895 MHz on LCP substrate). This observation can be easily corrected by scaling down the x-y dimensions of the antenna. In the paper case the antenna was scaled down by 87% while the antenna on PET by a factor of 92% and the new S_{11} results as shown in Fig. 14 were obtained. As seen in the figure, the detuning of the resonance can be easily performed by scaling the whole structure. For example, when placed on paper substrate, detuning becomes necessary if the thickness exceeds 1.5 mm.

As for the most common case where these RFID tags are placed on cardboard boxes; the dielectric properties of cardboard do not impede antenna characteristics due to its low dielectric constant (close to 1 and low loss properties [9]. However, the effect of the enclosed materials and the distance of the RFID tag from the arbitrarily placed enclosed contents play a more important role than the size and thickness of the cardboard. An alternative way to increase the bandwidth of the antenna in order to compensate for the material/fabrication variations is the use of a more broadband matching section, potentially introducing an additional stub-line.

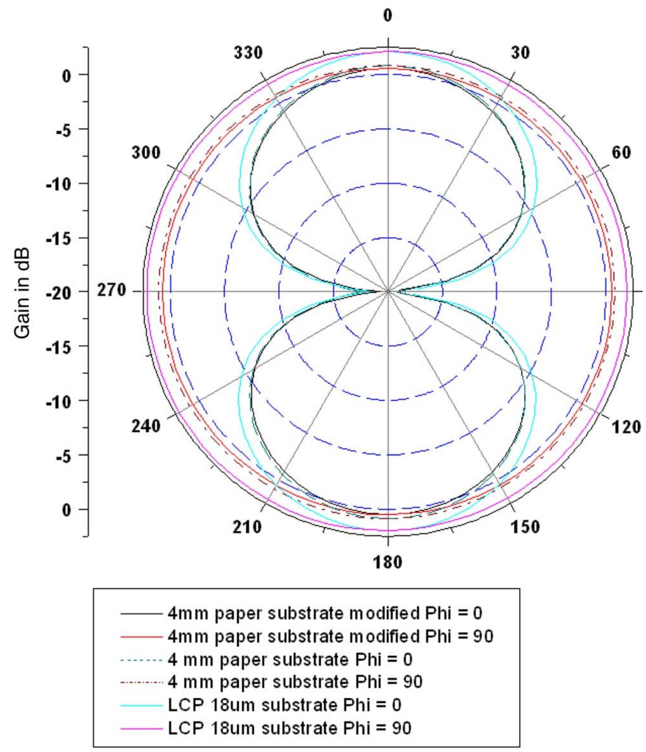

Fig. 15. Radiation pattern of the gain of the s-shaped antenna on paper, and LCP substrates.

In order to analyze the effect of the radiation pattern of these materials, the gain for the s-shaped antenna has been plotted in Fig. 15 for the LCP and paper substrates. The worst case scenario observed for gain loss was 1.049 dB (on 4 mm paper) for the E-plane or $\varphi = 0$ degrees plane in comparison with 2.095 dB (on 18 um LCP).

III. Inductively-Coupled Feed Structure

In the serial stub feed structure, the dimensions of the resistive shorting stub and the double inductive stub are comparable with the main radiating body. These stubs limit the miniaturization of the antenna size as a tradeoff for the enhanced bandwidth. For an ultra-compact RFID antenna design, a matching technique without any stubs is highly preferred. An inductively-coupled feed structure, similar to the one shown in Fig. 16, is such an effective way for impedance matching. The antenna consists of a feed loop with two terminals and a radiating body. The two terminals of the loop are connected to the IC, and the feed "communicates" with the antenna body through mutual coupling.

The inductively-coupled structure can be modeled as a transformer. Fig. 17 depicts the equivalent lumped element model, where R_{rb} and R_{loop} are the individual resistances of the radiating body and the feed loop. M is the mutual inductance and L_{loop} is the self-inductance of the feed loop. R_p and C_p are representing the substrate effects.

Compared with the serial stub feed structure in which off-resonance operation is preferred for better resistance/reactance stability, the inductively-coupled structure is designed at the resonant frequency. This is because at the resonant frequency f_0, assuming that the substrate effect is minimal, the components

Authorized licensed use limited to: Georgia Institute of Technology. Downloaded on November 29, 2009 at 22:44 from IEEE Xplore. Restrictions apply.

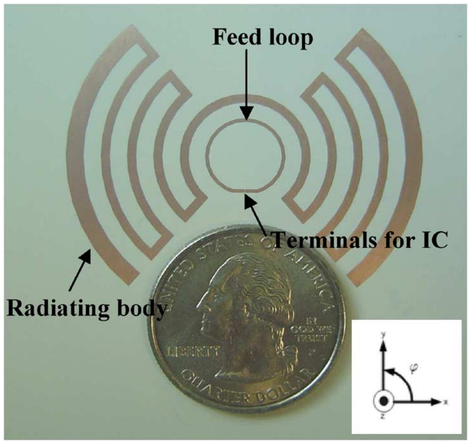

Fig. 16. Inductively coupled feed antenna fabricated on LCP substrate.

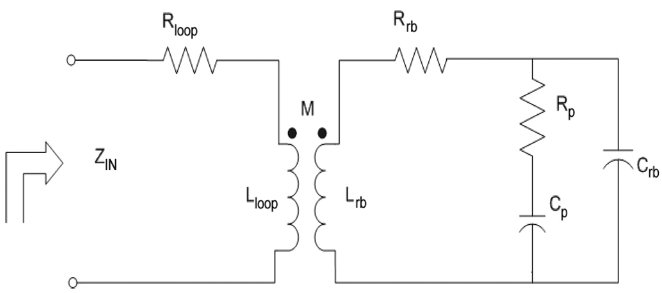

Fig. 17. Lumped element model for inductively coupled feeding RFID.

of antenna input resistance $\mathrm{R_{zin}}$ and reactance $\mathrm{X_{zin}}$ can be predicted as

$$R_{\mathrm{zin}} = \frac{(2\pi f_0 M)^2}{R_{rb}} + R_{\mathrm{loop}} \tag{1}$$

$$X_{\mathrm{zin}} = 2\pi f_0 L_{\mathrm{loop}}. \tag{2}$$

Thus, at the resonant frequency, the resistance is mainly controlled by M and $\mathrm{R_{rb}}$, and the reactance is dependent only upon $\mathrm{L_{loop}}$ [3]. In this way, the antenna input resistance and input reactance can be adjusted independently. Therefore, inductively coupled feeding structures present one of the theoretical optimum solutions to effectively match an antenna to arbitrary chip impedances, especially for RFID IC's with significant imaginary part.

An ultra-compact inductively-coupled feed antenna was designed in an area less than 1.7 in × 1.4 in, as illustrated in Fig. 12. The substrate was a flexible 4 mil LCP that has a dielectric constant ε_{r} of ~3.10 and a loss tangent $(\tan\delta)$ of 0.0019. Since the inductively-coupled feed structure is designed at the resonant frequency, the impedance response is sharper than the one in the serial stub structure, resulting in a narrower bandwidth. Therefore, the inductively-coupled antenna is more applicable to operate at specific bands. In this case, the antenna was designed to cover the European RFID band, ranging from 865–868 MHz. The target RFID chip impedance was 73 − j113 Ω. It has to be noted that the performance of this design is quite insensitive to fabrication tolerances and variations.

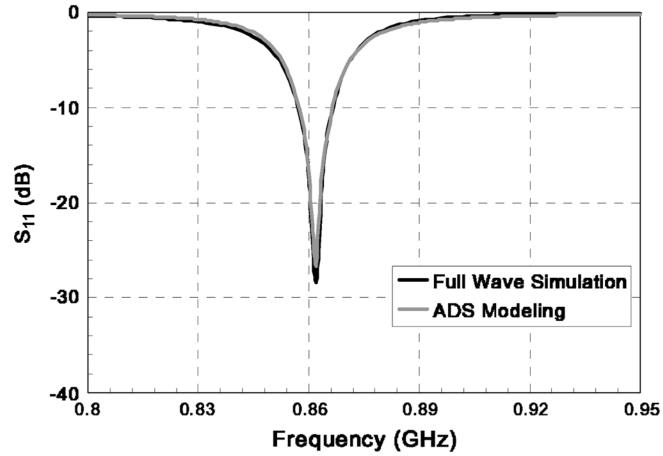

Fig. 18. Comparison of $\mathrm{S_{11}}$ full wave simulation results with ADS modeling.

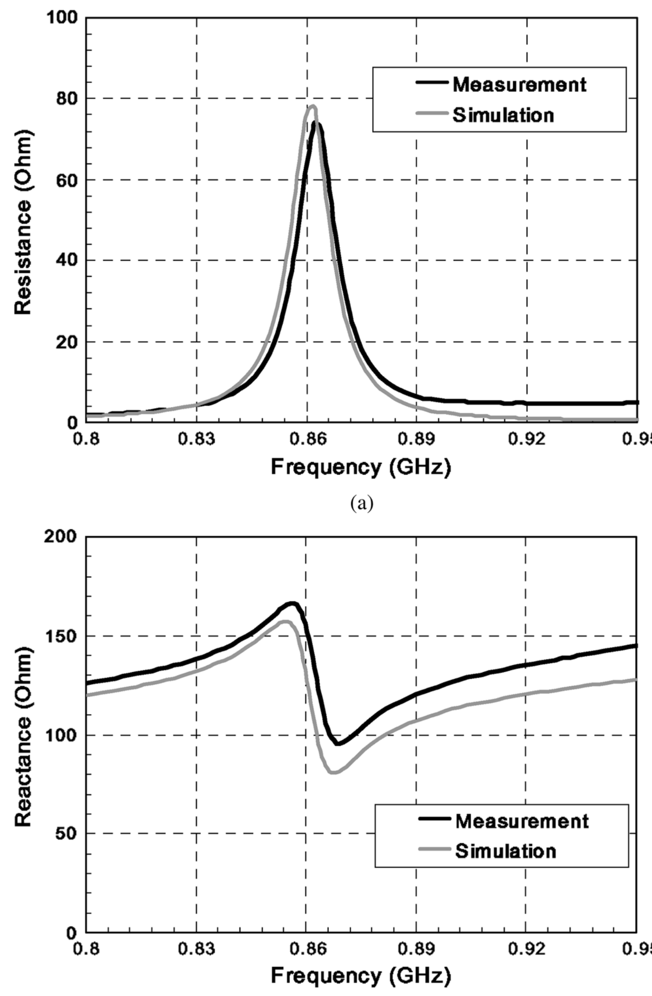

Fig. 19. Measured and simulated data of input impedance: (a) Resistance (b) Reactance.

The lumped element values of the equivalent circuit were optimized by ADS simulation software, including the substrate effects [10]. It can be seen that the model data and the full wave simulated impedance data demonstrate a very good agreement, as shown in Fig. 18.

Authorized licensed use limited to: Georgia Institute of Technology. Downloaded on November 29, 2009 at 22:44 from IEEE Xplore. Restrictions apply.

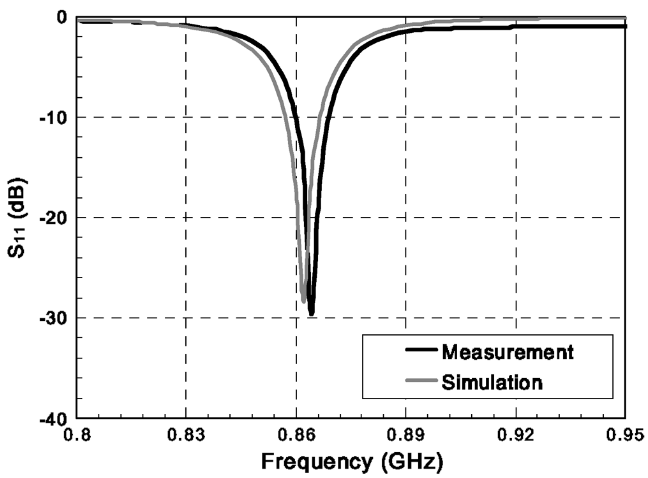

Fig. 20. S_{11} for measured and simulated data.

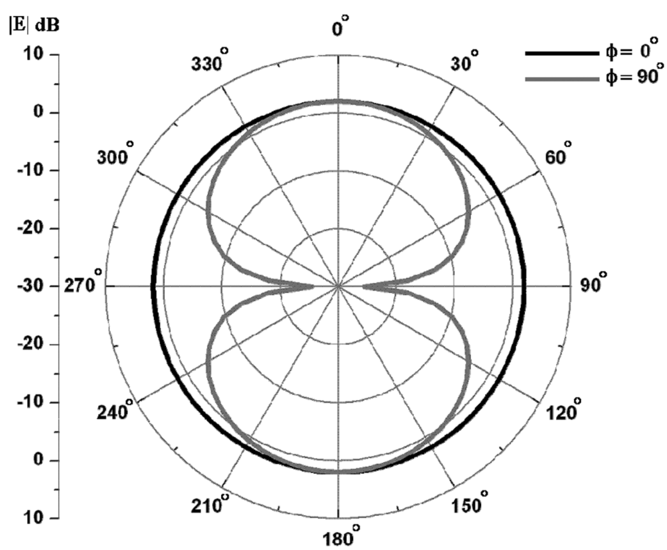

Fig. 21. 2D far-field radiation plot.

The measured and simulated input impedances of the antenna in the interested band are illustrated in Fig. 19 with a very good agreement. At 866 MHz, a measured input impedance of $60.8 + j102.5\ \Omega$ is achieved, resulting in a -30 dB reflection coefficient at that frequency. The S_{11} results below -10 dB extends from 858 MHz to 869 MHz, covering the whole European UHF band which extends from 865–868 MHz and accounting for most fabrication variations, as shown in Fig. 20.

Since the radiating body is basically a $\lambda/2$ dipole, the radiation pattern looks similar to the one of a dipole, as shown in Fig. 21. A directivity of 1.99 dBi is achieved with 90% radiation efficiency.

IV. Conclusion

This paper presents an overview of design requirements and novel approaches for improved performance UHF radio frequency identification (RFID) tags. Two matching techniques, an inductively coupled structure and a serial stub structure are discussed for the effective power transfer to/from the commonly used highly-capacitive IC's. Guidelines have been given for the design on common substrates and for any IC impedance by modifying the scale and the stubs respectively.

The serial stub matching method is highly preferable for multiband/multistandard RFIDs, while the inductively coupled matching method leads to ultra-miniaturized sizes (e.g., for healthcare applications). In addition, two approaches for antenna folding for optimum current flow and high radiation efficiencies (>90%) are also discussed. It has to be emphasized that both proposed antenna designs are quite insensitive to fabrication variations and offer maximized readability and range.

References

[1] K. Finkenzeller, *RFID Handbook*, 2nd ed. New York: Wiley, 2004.
[2] S. Basat, S. Bhattacharya, A. Rida, S. Johnston, L. Yang, M. M. Tentzeris, and J. Laskar, "Fabrication and assembly of a novel high-efficience UHF RFID tag on flexible LCP substrate," in *Proc. 56th IEEE-ECTC Symp.*, May 2006, pp. 1352–1355.
[3] H.-W. Son and C.-S. Pyo, "Design of RFID tag antennas using an inductively coupled feed," *Electron. Lett.*, vol. 41, no. 18, pp. 994–996, Sep. 2005.
[4] V. Subramanian and J. M. Frechet *et al.*, "Progress toward development of all-printed RFID tags: Materials, processes, and devices," *Proc. IEEE*, vol. 93, no. 7, pp. 1330–1338, Jul. 2005.
[5] S. Basat, S. Bhattacharya, L. Yang, A. Rida, M. M. Tentzeris, and J. Laskar, "Design of a novel high-efficiency UHF RFID antenna on flexible LCP substrate with high read-range capability," in *Proc. IEEE-APS Symp.*, Albuquerque, NM, Jul. 2006, pp. 1031–1034.
[6] P. V. Nikitin, S. Rao, S. F. Lam, V. Pillai, and H. Heinrich, "Power reflection coefficient analysis for complex impedances in RFID tag design," *IEEE Trans. Microw. Theory Tech.*, vol. 53, Sep. 2005.
[7] S. D. Kulkarni, R. M. Boisse, and S. N. Makarov, A Linearly-Polarized Compact UHF PIFA With Foam Support Dept. Electrical Eng., Worcester Polytechnic Inst..
[8] L. Yang, A. Rida, R. Vyas, and M. M. Tentzeris, "RFID tag and RF structures on a paper substrate using inkjet-printing technology," *IEEE Trans. Microw. Theory Tech.*, vol. 55, no. 12, pt. 2, pp. 2894–2901, Dec. 2007.
[9] J. D. Griffin, G. D. Durgin, A. Haldi, and B. Kippelen, "RF tag antenna performance on various materials using radio link budget," *IEEE Antennas Wireless Propag. Lett.*, Dec. 2006.
[10] L. Yang, S. Basat, and M. M. Tentzeris, "Design and development of novel inductively couple RFID antennas," in *Proc. IEEE-APS Symp.*, Albuquerque, NM, Jul. 2006, pp. 1035–1038.

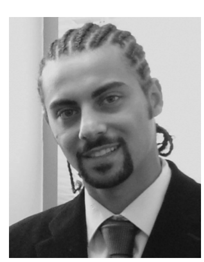

Amin H. Rida (S'05) received the B.S. and M.S. degrees in electrical engineering from the Georgia Institute of Technology, Atlanta, in May 2006 and May 2009, respectively, where he is currently working toward the Ph.D. degree.

He is currently with the Georgia Electronic Design Center (GEDC), Atlanta. His research interests include: design, development, and packaging of electronics (antennas, interconnects, 3D transitions, and integration) on organic, flexible, and high performance substrates for mm-wave frequencies. Other research topics focus on X-band filter design and Integration in a System on Package, characterization of organic substrates for RF applications, antenna design for RFID applications, and development of wireless transceivers for sensing and power scavenging applications.

Dr. Rida received the MTT-S Pre-graduate Scholarship in 2006 and the Best Student Paper Award at the IEEE Antennas and Propagation Symposium, Honolulu, HI, June 2007.

Authorized licensed use limited to: Georgia Institute of Technology. Downloaded on November 29, 2009 at 22:44 from IEEE Xplore. Restrictions apply.

Li Yang (S'05) received the B.S. and M.S. degrees in electronic engineering from Tsinghua University, Beijing, China, in 2002 and 2005, respectively. He is currently working toward the Ph.D. degree in electrical and computer engineering at the Georgia Institute of Technology, Atlanta.

He is a Graduate Research Assistant with the ATHENA Research Group, Georgia Electronic Design Center, Georgia Institute of Technology. His research interests include radio frequency identification (RFID) technology, radio frequency integrated circuit (RFIC) technology, and the design of high performance analog circuits for sensing and power scavenging applications.

Mr. Yang was the recipient/co-recipient of the 2008 IEEE IMS Student Paper Honorary Mention Award, the 2008 IEEE APS Symposium Student Paper Honorary Mention Award, the 2007 IEEE APS Symposium Best Student Paper Award, the 2007 IEEE IMS Third Best Student Paper Award, the 2007 ISAP Poster Presentation Award, and the 2006 Asian-Pacific Microwave Conference Award.

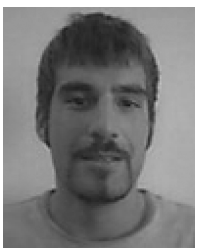

S. Serkan Basat received the B.S. (with highest honors) and M.S. degrees in electronic and computer engineering from the Georgia Institute of Technology, Atlanta, in 2003 and 2006, respectively.

He is currently working as an RF Engineer for Motorola Inc., Plantation, FL, where he is involved in product development for the Mobile Devices Division. He is member of a team working on RX/TX modules as well as Bluetooth.

Antonio Ferrer-Vidal received the Telecommunications Engineering degree from the UPV University, Valencia, Spain, in 2006.

Previously he participated in the research in the radio frequency identification (RFID) and antennas design areas in the ATHENA Group, Georgia Institute of Technology, Atlanta, as an Undergraduate Research Assistant and afterwards as a Research Engineer between 2005 and 2006 as part of a student exchange program between UPV and the Georgia Institute of Technology. At the moment he is working for a specialized RFID company based in Barcelona, Spain. His major responsibilities are managing and deploying active and passive RFID projects at a national and European scale.

Symeon (Simos) Nikolaou received the B.S.E.C.E. degree in electrical and computer engineering from the National Technical University of Greece (NTUA) Athens, Greece, in 2003 and the M.S.E.C.E. and Ph.D. degrees from the Georgia Institute of Technology (GaTech), Atlanta, in 2005 and 2007, respectively.

Since September 2007, he has been a Lecturer at Frederick University, Nicosia Cyprus and an Associate Researcher at the Frederick Research Center. He has authored or coauthored more than 25 publications in peer-reviewed journals and conferences. His research interests include the design of UWB, conformal and reconfigurable antennas, compact RFIDs and reconfigurable filters on organic materials

Manos M. Tentzeris (SM'98) received the Diploma Degree in Electrical and Computer Engineering from the National Technical University of Athens (*magna cum laude*) in Greece and the M.S. and Ph.D. degrees in Electrical Engineering and Computer Science from the University of Michigan, Ann Arbor, MI.

He is currently a Professor with School of Electrical and Computer Engineering, Georgia Institute of Technology, Atlanta. He has published more than 320 papers in refereed journals and conference proceedings, three books and 17 book chapters. He has helped develop academic programs in highly integrated/multilayer packaging for RF and wireless applications using ceramic and organic flexible materials, paper-based RFID's and sensors, microwave MEM's, SOP-integrated (UWB, multi-band, conformal) antennas and adaptive numerical electromagnetics (FDTD, multiresolution algorithms) and heads the ATHENA Research Group (20 researchers). He is the Georgia Electronic Design Center Associate Director for RFID/Sensors research, and he has been the Georgia Tech NSF-Packaging Research Center Associate Director for RF Research and the RF Alliance Leader from 2003–2006. He was a Visiting Professor with the Technical University of Munich, Germany for the summer of 2002, where he introduced a course in the area of high-frequency packaging.

Prof. Tentzeris is a member of URSI-Commission D, a member of MTT-15 committee, an Associate Member of EuMA, a Fellow of the Electromagnetic Academy and a member of the Technical Chamber of Greece. He was the recipient/co-recipient of the 2007 IEEE APS Symposium Best Student Paper Award, the 2007 IEEE IMS Third Best Student Paper Award, the 2007 ISAP 2007 Poster Presentation Award, the 2006 IEEE MTT Outstanding Young Engineer Award, the 2006 Asian-Pacific Microwave Conference Award, the 2004 IEEE TRANSACTIONS ON ADVANCED PACKAGING Commendable Paper Award, the 2003 NASA Godfrey "Art" Anzic Collaborative Distinguished Publication Award, the 2003 IBC International Educator of the Year Award, the 2003 IEEE CPMT Outstanding Young Engineer Award, the 2002 International Conference on Microwave and Millimeter-Wave Technology Best Paper Award (Beijing, CHINA), the 2002 Georgia Tech-ECE Outstanding Junior Faculty Award, the 2001 ACES Conference Best Paper Award and the 2000 NSF CAREER Award and the 1997 Best Paper Award of the International Hybrid Microelectronics and Packaging Society. He was the TPC Chair for IEEE IMS 2008 Symposium and the Chair of the 2005 IEEE CEM-TD Workshop and he is the Vice-Chair of the RF Technical Committee (TC16) of the IEEE CPMT Society. He is the founder and chair of the RFID Technical Committee (TC24) of the IEEE MTT Society and the Secretary/Treasurer of the IEEE C-RFID. He has organized various sessions and workshops on RF/Wireless Packaging and Integration, RFID's, Numerical Techniques/Wavelets, in IEEE ECTC, IMS, VTC and APS Symposia in all of which he is a member of the Technical Program Committee in the area of "Components and RF." He is an Associate Editor of the IEEE TRANSACTIONS ON MICROWAVE THEORY AND TECHNIQUES, IEEE TRANSACTIONS ON ADVANCED PACKAGING and *International Journal on Antennas and Propagation*. He has given more than 50 invited talks in the same area to various universities and companies in Europe, Asia and America.

Authorized licensed use limited to: Georgia Institute of Technology. Downloaded on November 29, 2009 at 22:44 from IEEE Xplore. Restrictions apply.